Catal Lett (2008) 121:274–282
DOI 10.1007/s10562-007-9329-9

Preparation of Catalyst Ni–Cu/CNTs by Chemical Reduction with Formaldehyde for Steam Reforming of Methanol

Ping-Heng Liao · Hung-Ming Yang

Received: 14 September 2007 / Accepted: 19 October 2007 / Published online: 8 November 2007

Abstract The novel catalyst Ni–Cu alloys supported on carbon nanotubes (CNTs) was prepared by reduction with formaldehyde and applied in steam reforming of methanol. With nitric acid and sulfuric acid to create defects on the surface of CNTs and using ethanol to improve the hydrophilicity of CNTs, the Ni–Cu alloys were anchored on the surface of CNTs by co-reduction of Ni- and Cu-precursors under the use of tetra-n-methylammonium hydroxide to reduce the aggregation of Ni–Cu particles. In contrast, Ni–Cu catalyst supported on activated carbon (Ni–Cu/C) was prepared as well, and the bimetal of Ni and Cu supported on CNTs (Ni/Cu/CNTs) was attained by successive reduction of first Cu- and then Ni-precursors. The catalysts were characterized with XRD, ED, FESEM, transmission electron microscopy, and Thermogravimetric analysis. The hydrogen yield in steam reforming of methanol was near 100% at 360 °C over 20 wt.% Ni_{20}–Cu_{80}/CNTs. The catalytic activity of Ni_{20}–Cu_{80}/CNTs is much higher than that of Ni_{20}–Cu_{80}/C and Ni_{20}/Cu_{80}/CNTs.

Keywords Hydrogen production · Carbon nanotubes · Ni–Cu alloys · Chemical reduction · Steam reforming of methanol

1 Introduction

Methanol, compared to natural gas or other hydrocarbons, is a more efficient energy source to produce hydrogen used in fuel cells. In general, there are three methods to generate hydrogen from methanol, i.e., partial oxidation, decomposition, and steam reforming [1–3]. Considering the route of steam reforming, catalysts commonly used are Cu, Ni, Zn, Cr, Pd, Rh, Pt, and elements in group VIII [4, 5]. Wang et al. [6] and Alejo et al. [3] utilized Cu-based catalysts containing a binary or ternary metal to catalyze partial oxidation of methanol. They obtained the higher conversion of methanol and selectivity of hydrogen by using $Cu_{60}Cr_{40}$ catalysts, as compared with other bimetallic catalysts and catalysts that contain Zn promoter. Suetsuna et al. [7] reported a monolithic Cu–Ni catalyst embedded in (Ni, Mg)O ceramic substrate to conduct CO_2 reforming of methane and steam reforming of methanol, and found that the catalysts had a higher reforming activity which was mainly attributed to the dispersed Cu–Ni nano-particles.

The support of catalysts plays an important role in catalysis. SiO_2 and Al_2O_3 [8, 9], the materials MCM-41, carbon black, honeycomb of ceramics can be utilized as efficient supports [10–12]. Recently, carbon nanotubes (CNTs) were also applied as the support of catalysts due to their special structural morphology and characteristics [13]. When used as the support, the surface of CNTs is usually modified to create functional groups for specific needs. Catalysts supported on CNTs have been prepared by impregnation [14–15], precipitation [16], colloidal, electroless plating [17], and hydrothermal method [18]. Liu et al. [19] successfully prepared the catalyst Ni/CNTs by electroless plating for the synthesis of new CNTs. Currently, one of the main challenges for applications of CNTs might be the high cost, as well as the industrial scale of production achieved by chemical vapor deposition (CVD). However, using CNTs as the support of catalysts seems to be effective and attractive due to its increasingly widespread applications.

P.-H. Liao · H.-M. Yang (✉)
Department of Chemical Engineering, National Chung Hsing University, 250 Kuo-kuang Road, Taichung 402, Taiwan, ROC
e-mail: hmyang@dragon.nchu.edu.tw

In this work, an effective catalyst of Ni–Cu alloys supported on CNTs by co-reduction of Ni- and Cu-precursors with formaldehyde is prepared and applied in steam reforming of methanol for producing hydrogen. The order of reduction reactions of metal-precursors affects the catalytic activity. Hence, a bimetallic catalyst supported on CNTs was also prepared by successive reduction of Cu- and Ni- precursors. In contrast, the catalyst Ni–Cu alloys supported on activated carbon was prepared by the similar procedures. The catalytic performance of Ni/CNTs, Cu/CNTs, Ni–Cu/CNTs, Ni/Cu/CNTs, and Ni–Cu/C in steam reforming of methanol was discussed.

2 Experimentals

2.1 Preparation of Catalysts

Two different types of catalyst supported on CNT were prepared. The term 'Ni–Cu' is defined as alloy formed by co-reduction of Ni- and Cu- precursors; while 'Ni/Cu' means that the bimetal of Ni and Cu are prepared by successive reduction of first Cu-precursor and then Ni-precursor. The commercial multi-walled CNTs with tube diameters of about 30–60 nm, 95% in purity and 50.2 m^2/g of BET surface area were purchased from Desunnano Co., Ltd. in Taiwan. The activated carbon powder (95+% in purity and 920.5 m^2/g of BET surface area) was purchased from SHOWA Chemical Co., Ltd. To modify the surface of CNTs, one gram of CNTs was introduced into a 40 cm^3 of acid-solution (60 wt.% nitric acid to 97 wt.% sulfuric acid = 3/1 in volume); then 10 cm^3 of ethanol were dripped into the solution slowly. The solution was agitated in a shaker at 70 °C and 150 rpm for 24 h to enhance the hydrophilicity of CNTs. The BET surface area of CNTs after acid-treatment was measured to be 64.0 m^2/g. To load Ni–Cu on the surface of CNTs, the metal precursors, 0.01 M of $Cu(NO_3)_2$ $3H_2O$, and 0.01 M of $Ni(OOC_2H_3)_2$ $4H_2O$, were introduced into a solution which was prepared by mixing 99% of ethanol and an aqueous solution (0.01 M of NaOH and Na_2CO_3, pH = 12) in equal volume. Tetramethylammonium hydroxide (TMAOH, 25 wt.% solution) in a molar quantity of one fifth of metal precursors and 0.2 g of acid-treated CNTs were added into the solution. The co-reduction of Ni and Cu precursors was started by dripping formaldehyde (37% solution) in a molar ratio of 20 (formaldehyde to metal precursors) for 1 h under ultrasonic shaking. After the reduction reaction, the solids were separated from the solution with a filter. After that, de-ionized water was used to wash the solids, and then the solid-water mixture was filtrated until a pH-value around 7 in the filtrate was reached. The solid samples were separated with centrifuging and dried at 105 °C for 4 h, and then calcined at 350 °C for 0.5 h with 80 cm^3/min of nitrogen. After calcination, the samples were reduced with hydrogen (15 cm^3/min) in 80 cm^3/min of nitrogen at 260 °C for 30 min. The catalyst Ni–Cu/CNTs with a BET surface area of 66.6 m^2/g was attained. Instead of co-reduction of Cu and Ni precursors, a bimetallic catalyst Ni/Cu/CNTs was prepared under the same conditions as described above, except with the introduction and reduction of first Cu then Ni. The preparative procedures of Ni–Cu supported on activated carbon (Ni–Cu/C) were the same with that of Ni–Cu/CNTs.

2.2 Characterization of Catalysts

The crystal phase present in catalysts was determined by X-ray powder diffraction (XRD) operating with 40 kV of voltage and 30 mA of tube current to obtain Cu-Kα radiation (wave length = 1.54056 Å) and with 2θ scanning from 20° to 80°; the phase identification was performed using the reference database (JCPDS-files). The particle size and distribution of metals in catalysts were observed with an analytical electron microscope (JEOL JEM-1200CX II), for which the catalyst sample was grinded and dispersed in isopropyl alcohol in an ultrasonic bath for 15 min, and then coated on a carbon-coated copper screen. After evaporating isopropyl alcohol, the sample was analyzed with transmission electron microscopy (TEM). The elements of samples were identified with Energy Dispersive Spectrometer (EDS). The electron diffraction (ED) pattern was also used to identify the crystal lattice of metals supported on CNTs. Thermogravimetric analysis (TGA) was employed to determine the actual loading of metals and to analyze thermal properties of the catalysts. In the experiments of TGA, the sample was heated by air from 100 to 900 °C under a temperature increase of 10 °C/min.

2.3 Reactor System

An isothermal fixed-bed tubular reactor packed with 0.2 g of catalyst was used to carry out steam reforming of methanol. The reactor was a stainless steel pipe of 3.5 cm in length and 1/4 in. in diameter. Two thermocouples were set at the entrance and exit of the reactor to measure the reaction temperature. The liquid reactants, water and methanol at the desired molar ratio, were well mixed in an ultrasonic bath for 1 h and preheated to 60 °C, then continuously fed to the reactor at desired flow rate. To ensure a flow of gas stream within the entire reactor system, the temperature on all pipes was kept above 120 °C. The steam reforming reaction was carried out at atmospheric pressure and at a temperature in the range of 200–400 °C with

dilution gas N_2 at a flow rate of 80 cm^3/min. The exit stream was analyzed by online gas chromatography (with packed column and TCD) using argon as carrier gas. The yield of H_2, conversion of CH_3OH and selectivity of CO_2 were defined by the formulas,

$$\text{yield of } H_2: Y_{H_2} = \frac{F_{H_2}}{3 \times F_{CH_3OH,0}} \times 100\%,$$

$$\text{conversion of } CH_3OH: X_{CH_3OH} = \frac{F_{CO_2} + F_{CO}}{F_{CH_3OH,0}} \times 100\%,$$

$$\text{selectivity of } CO_2: S_{CO_2} = \frac{F_{CO_2}}{F_{CO} + F_{CO_2}} \times 100\%,$$

where F_{H_2} = molar flow rate of H_2 (mol/min), F_{CO} = molar flow rate of CO (mol/min), F_{CO_2} = molar flow rate of CO_2 (mol/min), and $F_{CH_3OH,0}$ = feeding rate of CH_3OH (mol/min).

3 Results and Discussion

3.1 Characterization of Catalysts

Since CNTs are hydrophobic materials, an acid-treatment to make defects on the surface of CNTs is necessary for creating functional groups on it, such as hydroxyl, carboxyl, and carbonyl [20, 21]. After that, the BET surface area of CNTs was increased from 50.2 to 64.0 m^2/g, and the oxidation temperature was raised from 570 to 645 °C. The addition of a suitable amount of ethanol improves the hydrophobic CNTs more accessible to the metal precursors by regulating the polarity of the aqueous solution; thus Ni^{2+} and Cu^{2+} can be properly reduced to form alloys of Ni–Cu on the surface of CNTs.

Table 1 is the results of TGA for different loadings of metals in Ni_{20}–Cu_{80}/CNTs. Based on the weight % of residual in TGA experiments, the actual loading of metals on CNTs was estimated. From TGA analysis, the impurities existing on the surface of CNTs were reduced from 2.5 to 1.4 wt.% by the acid-treatment. The real loadings of metals all corresponded to desired amounts with deviations <2 wt.%, and the oxidation temperatures of CNTs would be reduced from 645 °C to the range of 505–520 °C after supporting Ni–Cu particles. The Ni–Cu alloys may act as catalysts for oxidation of carbon to reduce the oxidation temperature. Hence, such a reduction in oxidation temperature might be resulted from the Ni–Cu alloys acting as catalysts for oxidation of CNTs and destroying the surface of CNTs.

The quaternary ammonium salts, tetra-*n*-butylammonium bromide (TBAB) and TMAOH, used as dispersant during the chemical reduction reaction are discussed. Figure 1 shows the FESEM analysis for the effect of dispersants on 15 wt.% Ni/CNTs, Fig. 1a for TBAB and Fig. 1b for TMAOH. From Fig. 1a, the particle sizes of Ni were about 10–15 nm and some particles were aggregated to a size larger than 100 nm. By using TMAOH as dispersant, a better distribution of Ni particles was observed and the particle sizes were about 10–20 nm. It might be that TMAOH has smaller molecular size and higher hydrophilicity than TBAB does, and makes Ni particles distributed more efficiently.

Figure 2 shows the XRD patterns for 20 wt.% Ni and different loadings (6–28 wt.%) of Ni_{20}–Cu_{80} alloys supported on CNTs. Apparently, Ni–Cu alloys can be formed and loaded on the surface of CNTs by co-reduction of Ni- and Cu- precursors. The intensities of peaks of Ni–Cu alloys, as shown in (b–e) of Fig. 2, reveal that the actual loading of Ni–Cu alloys decreased with the decrease of amounts of metals employed. The particle sizes of Ni and Ni–Cu alloys can be calculated using Scherrer's equation, $D_{XRD} = \alpha\lambda/B\cos\theta$, with $\alpha = 0.90$, $\lambda = 0.154$ nm, B = half of integral breadth; the D_{111}-values are calculated as 15.0 nm for 20 wt.% Ni/CNTs, 15.4 nm for 28 wt.% Ni_{20}–Cu_{80}/CNTs, 15.9 nm for 15 wt.% Ni_{20}–Cu_{80}/CNTs, 10.8 nm for 10 wt.% Ni_{20}–Cu_{80}/CNTs, and 8.6 nm for 6 wt.% Ni_{20}–Cu_{80}/CNTs. The particle sizes of Ni–Cu alloys were about 15 nm when the loading of metals was >15 wt.%, and became smaller if the loadings were <10 wt.%. The ED pattern for 28 wt.% Ni_{20}–Cu_{80}/CNTs confirms the formation of Ni–Cu alloys on the surface of CNTs by reduction with formaldehyde, as shown in Fig. 3a. The crystal lattices can be identified from the concentric bright rings with occasional bright spots. As shown in Table 2, the d-spacings and the diameters of the concentric bright rings are measured as 2.08 Å and

Table 1 TGA analysis for different loadings of metals on Ni_{20}–Cu_{80}/CNTs

Ni_{20}–Cu_{80} content (wt.%)	Oxidation temperature of carbon nano-tubes (°C)	Residual weight % by TGA (wt.%)	Loading of Ni_{20}–Cu_{80}[a] (wt.%)
28	505	33.5	25.53
20	515	27.0	21.41
15	513	20.7	15.35
10	518	14.7	10.58
6	520	8.2	5.41
0[b]	645	1.4	0
0[c]	570	2.5	0

[a] Calculated from loading of NiO and CuO by TGA

[b] CNTs with acid-treatment

[c] CNTs without acid-treatment

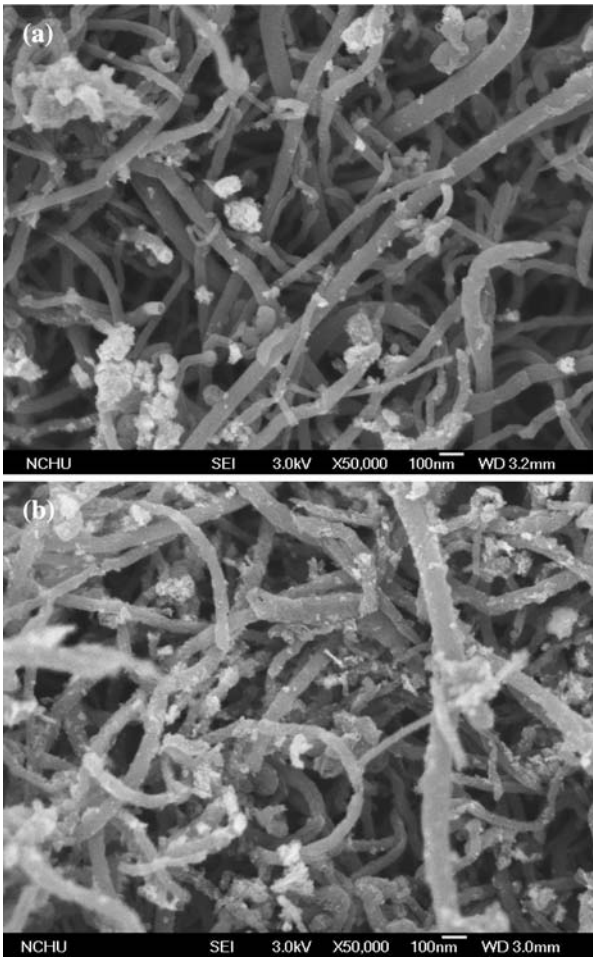

Fig. 1 FESEM micrographs of 15 wt.% Ni/CNTs for the effect of dispersants. Preparation conditions: acid-treated CNTs, 30.6 cm^3 of 0.01 M $Ni(OOC_2H_3)_2$, 20 of molar ratio of formaldehyde to $Ni(OOC_2H_3)_2$, 15 cm^3 of ethanol, 15 cm^3 of basic solution. Dispersants: (**a**) TBAB, (**b**) TMAOH

1.61 cm for Ni–Cu (111), 1.81 Å and 1.89 cm for Ni–Cu (200), 1.28 Å and 2.68 cm for Ni–Cu (220), 1.08 Å and 3.15 cm for Ni–Cu (311), respectively, in a ratio of square of the radius (or diameter) of the concentric rings to be 3:4:8:11, which is in agreement with that of Ni–Cu alloys [22]. Figure 3b shows the TEM image of 28 wt.% Ni_{20}–Cu_{80}/CNTs, exhibiting 16 nm of average particle size and some particles aggregated. The elements of 20 wt.% Ni_{20}–Cu_{80}/CNTs were identified with EDS analysis, as shown in Table 3. The elemental weight ratio of Ni to Cu was close to 1:4, and the weight percentage of alloys was about 20 wt.%.

3.2 Steam Reforming Reaction of Methanol

The prepared catalysts were applied in the steam reforming of methanol in a fixed-bed reactor for hydrogen production.

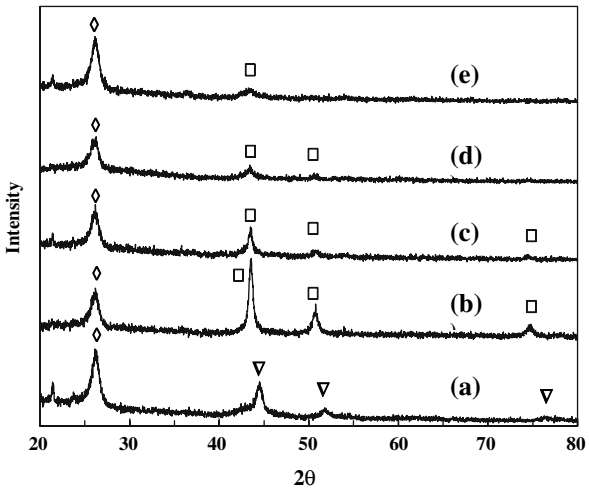

Fig. 2 XRD analysis of reduced samples. (**a**) 20 wt.% Ni/CNTs, (**b**) 28 wt.% Ni_{20}–Cu_{80}/CNTs, (**c**) 15 wt.% Ni_{20}–Cu_{80}/CNTs, (**d**) 10 wt.% Ni_{20}–Cu_{80}/CNTs, (**e**) 6 wt.% Ni_{20}–Cu_{80}/CNTs. Symbol: (*open diamond*) CNT, (*open upside down triangle*) Ni, (*open square*) Ni–Cu alloy

The reaction conditions were set at 0.2 g of catalysts, 30.5 h of WHSV, 7 cm^3/h of volumetric flow rate of a liquid mixture of water and methanol (designated as Q), different molar ratios of water to methanol (designated as *M*-value), and 80 cm^3/min of the dilution gas nitrogen.

The structure, adsorptive ability and thermal properties of the supports would affect the dispersion and particle size of metals as well as the catalytic activity. In comparison with other carbonaceous supports, a catalyst of Ni–Cu alloys supported on activated carbon was also prepared and applied in the steam reforming reaction. As shown in Fig. 4, the catalytic activity of Ni_{20}–Cu_{80}/CNTs is much higher than that of Ni_{20}–Cu_{80}/C. However, these two catalysts had similar behaviors in selectivity of CO_2 within the range of 53–85% at 200–400 °C. Figure 5 is the images of FESEM for using CNTs and activated carbon as the supports, Fig. 5a for CNTs and Fig. 5b for C. As shown in Fig. 5a, b, better metallic distribution and lower aggregation of metal particles were observed by using CNTs as supports than using activated carbon as supports. For activated carbon, the Ni–Cu alloys migrated and aggregated to form bigger particles; that made the activity of Ni–Cu/C reduced significantly in spite of the large surface area of C. In contrast, considering the specific structures of CNTs, they have a large ratio of length to diameter, the honeycomb-like arrangement of carbon atoms in the graphite sheets, and appropriate pore-size distribution. These properties make CNTs capable of providing a better environment to distribute the anchoring metals. Table 4 shows the comparison of activity on the basis of TOF in steam reforming of methanol for 20 wt.% Ni_{20}–Cu_{80}/CNTs, 20 wt.% Ni_{20}/Cu_{80}/CNTs, and 20 wt.% Ni_{20}–Cu_{80}/

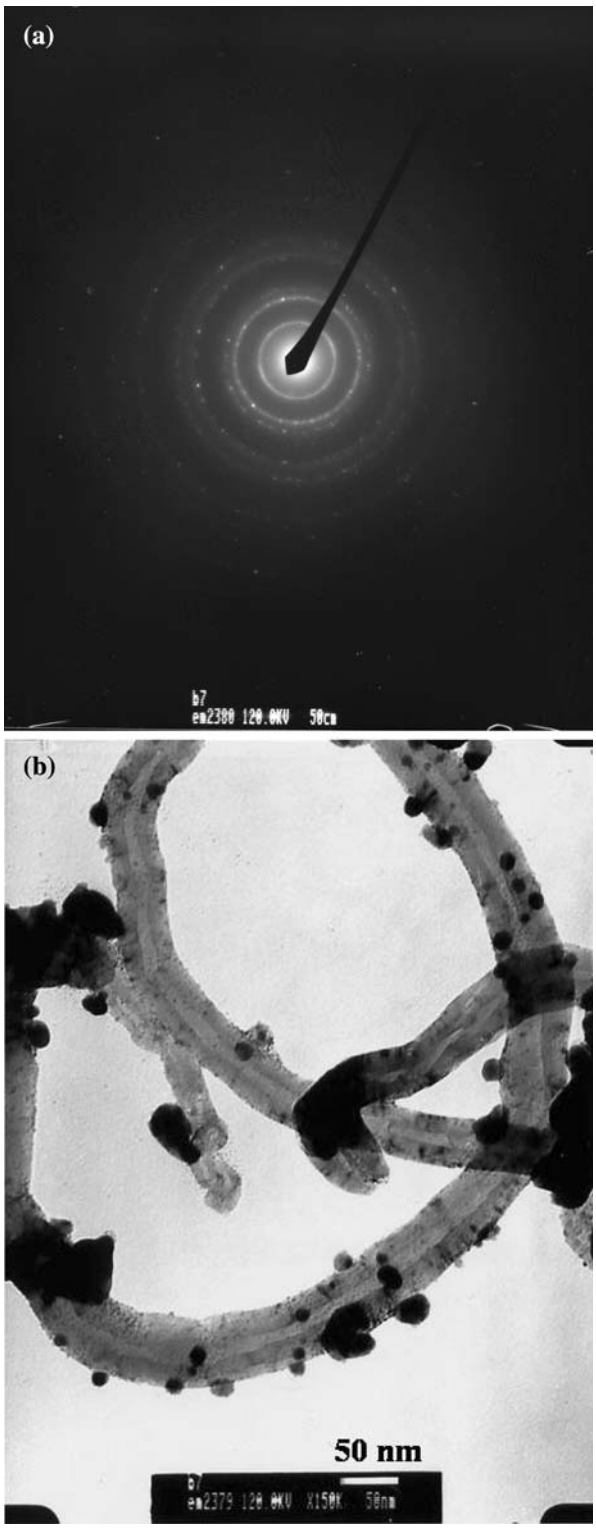

Fig. 3 ED and TEM analysis of 28 wt.% Ni_{20}–Cu_{80}/CNTs: (**a**) ED pattern, (**b**) TEM micrograph

C. Among the three catalysts, Ni_{20}–Cu_{80}/CNTs had the highest activity with 98.7% of H_2 yield at 360 °C. The order of TOF for tested catalysts is Ni_{20}–Cu_{80}/CNTs > Ni_{20}/Cu_{80}/CNTs > Ni_{20}–Cu_{80}/C. Also compared with the conventional catalysis, the hydrogen production rate over 20 wt.% Ni_{20}–Cu_{80}/CNTs catalyst was above 400 mmol H_2 kg_{cal}/s, which is higher than that over 12 wt.% Cu/Zn/γ-Al_2O_3 (about 160 mmol H_2kg_{cal}/s) [23].

The addition of dispersant affects the distribution of metals on the surface of CNTs, and that in turn affects the catalytic activity. In this work, TMAOH was employed as

Table 2 Analysis of Ni–Cu alloys supported on CNTs by electron diffraction pattern

Materials	D-spacing (Å)	Radius[a] (cm)	Diameter[a] (cm)	Diameter[b] (cm)
Ni–Cu alloy	2.08	0.81	1.62	1.61
	1.79	0.94	1.88	1.89
	1.26	1.33	2.66	2.68
	1.08	1.56	3.12	3.15
CNTs	3.37	0.50	1.00	1.00
	2.13	0.79	1.59	1.60

[a] Calculated by the formula $Rd = \lambda L$, R: radius, d: D-spacing, λ (wave length): 0.03384 Å, L (camera length): 50 cm

[b] Measured from Fig. 3a by vernier

Table 3 EDS analysis for 20 wt.% Ni_{20}–Cu_{80}/CNTs

Element	Weight (%)	Atomic (%)
C	77.50	94.71
Ni	4.84	1.21
Cu	17.66	4.08
Total	100	100

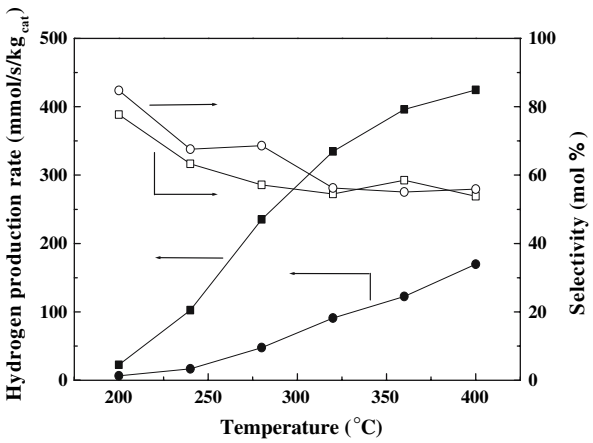

Fig. 4 Comparison of Ni_{20}–Cu_{80}/CNTs and Ni_{20}–Cu_{80}/C on steam reforming of methanol; 20 wt.% of metal loading, 30.5 h of WHSV, 7 cm^3/h of Q, 1.5 of M, temperature at 200–400 °C, 80 cm^3/min of volumetric rate of nitrogen; H_2 production rate for (*filled square*) Ni_{20}–Cu_{80}/CNTs, and (*filled circle*) Ni_{20}–Cu_{80}/C; selectivity of CO_2 for (*open square*) Ni_{20}–Cu_{80}/CNTs, (*open circle*) Ni_{20}–Cu_{80}/C

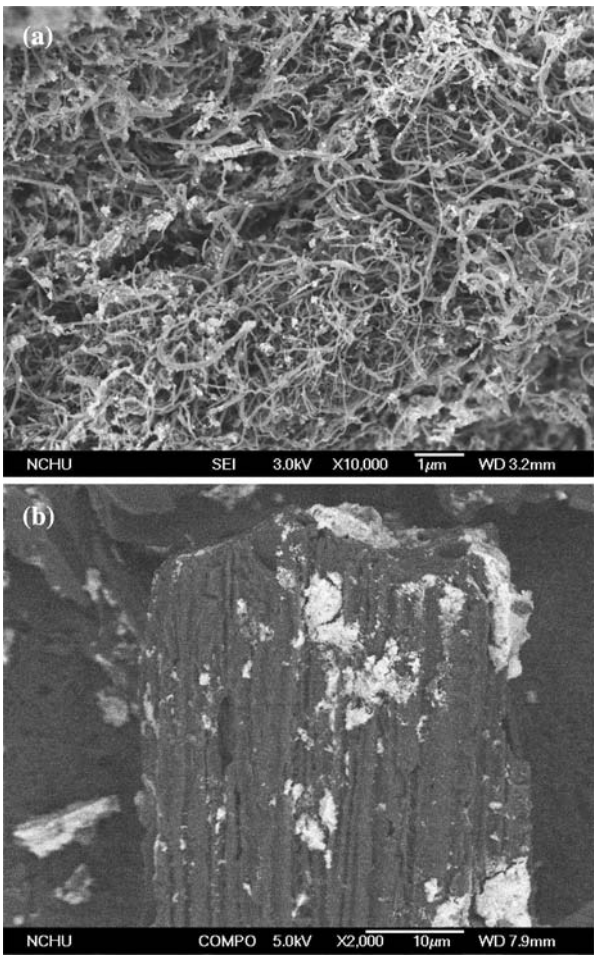

Fig. 5 FESEM micrographs of (**a**) 20 wt.% Ni_{20}–Cu_{80}/CNTs and (**b**) 20 wt.% Ni_{20}–Cu_{80}/C. Preparation conditions: 0.2 g of acid-treated CNTs and C, 80 cm^3 of 0.01 M $Ni(OOC_2H_3)_2$ and $Cu(NO_3).3H_2O$ in molar ratio of 1/4, 20 of molar ratio of formaldehyde to $Ni(OOC_2H_3)_2$ and $Cu(NO_3).3H_2O$, 40 cm^3 of ethanol, 40 cm^3 of basic solution. Dispersants: TMAOH

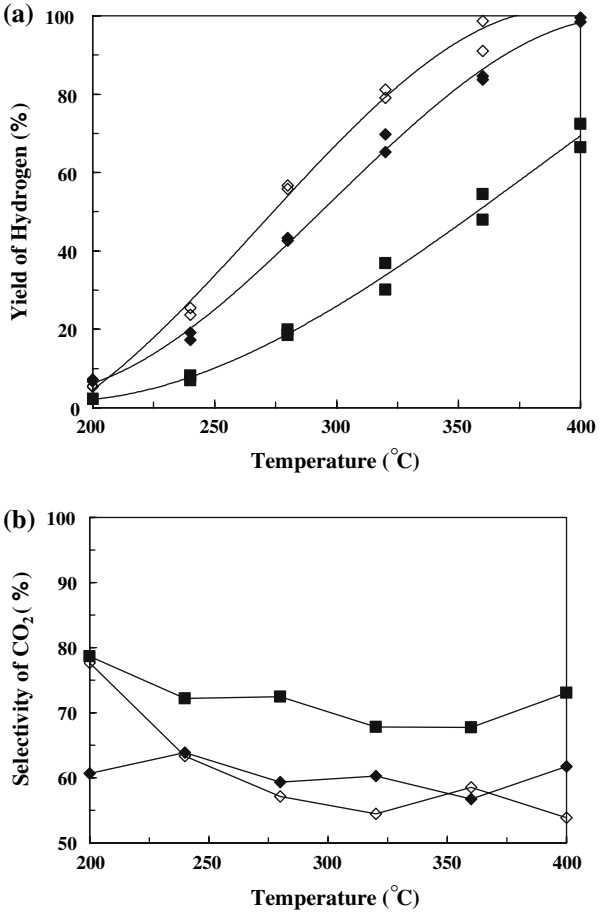

Fig. 6 Effect of TMAOH on the activity of catalyst: (**a**) hydrogen production, (**b**) selectivity of CO_2, 30.5 h of WHSV, 7 cm^3/h of Q, 1.5 of M, temperature at 200–400 °C, 80 cm^3/min of volumetric rate of nitrogen, 20 wt.% of loading of metals; (*filled square*) Ni/CNTs (without TMAOH), (*filled diamond*) Ni/CNTs (with TMAOH), (*open diamond*) Ni_{20}–Cu_{80}/CNTs (with TMAOH)

Table 4 Comparisons of activity of supported catalysts in steam reforming of methanol[a]

Catalysts	H_2 yield (%)	H_2 production rate (mmol H_2 s^{-1} kg_{cat}^{-1})	Selectivity of CO_2 (%)	TOF[b] (10 s)
Cu_{20}–Ni_{80}/CNTs	98.7	412.1	58.5	16.3
Cu_{20}/Ni_{80}/CNTs	75.3	333.2	62.2	8.8
Cu_{20}–Ni_{80}/C	30.2	125.9	55.1	5.0

[a] Reaction conditions: 0.2 g of catalyst (20 wt.% of metal content), 30.5 h of WHSV, 7 cm^3/h of Q, 1.5 of M, temperature at 360 °C, 80 cm^3/min of volumetric rate of nitrogen

[b] Hydrogen production per surface copper atom per second

the dispersant. Figure 6 shows the effect of 20 wt.% of loading of metals in catalysts prepared with or without TMAOH on the hydrogen production rate and the selectivity of CO_2 at different reaction temperatures. The tested catalysts were Ni/CNTs (without TMAOH), Ni/CNTs (with TMAOH), and Ni_{20}–Cu_{80}/CNTs (with TMAOH). The hydrogen yields in steam reforming of methanol for the three catalysts are shown in Fig. 6a. The hydrogen yields for catalysts prepared with TMAOH were greater than that without TMAOH. Among the three tested catalysts, Ni_{20}–Cu_{80}/CNTs (with TMAOH) presented the highest catalytic activity. A larger enhancement appeared at 400 °C indicates the distribution of metals affects the activity of catalyst; from the result in Fig. 1, a better metal distribution with TMAOH was also observed. Therefore, the catalyst has better activity when preparing catalysts with TMAOH as dispersant. In addition, as shown in Fig. 6b, the selectivity of CO_2 for Ni/CNTs (with TMAOH) was lower than that without TMAOH. Considering the reactions that occur in steam reforming of methanol:

$CH_3OH + H_2O = 3H_2 + CO_2$ (methanol steam reforming, MSR),

$CH_3OH = 2H_2 + CO$(methanol decomposition, MD),

$CO + H_2O = CO_2 + H_2$(water - gas shift, WGS),

the MSR reaction proceeds much faster than MD over a Cu-based catalyst [24]; while a better distribution of Ni particles would induce a faster rate of MD reaction to result in an increase of CO. This confirms that TMAOH is an effective dispersant for preparing catalysts supported on CNTs.

The Cu-based catalysts favored the MSR and WGS reactions more than MD reaction; however, MD reaction might still occur in a minor at a high temperature, and CO might be produced by the RWGS reaction [1, 24]. Figure 7 shows the molar fraction of methanol, hydrogen, carbon monoxide and carbon dioxide in exit gas as a function of temperature using 20 wt.% Ni_{20}–Cu_{80}/CNTs. The conversion of methanol reached 100% at about 360 °C, and the selectivity of CO_2 was 50–75%. At a lower temperature the selectivity of CO_2 was greater than 75% and decreased gradually with increasing temperature. This implies that MSR and WGS reactions were faster than MD reaction at a lower temperature. The MD and RWGS reactions became significant as the temperature raised.

Figure 8 shows the comparison of catalytic performance between Ni_{20}/Cu_{80}/CNTs and Ni_{20}–Cu_{80}/CNTs. The results demonstrate that Ni_{20}–Cu_{80}/CNTs had a higher activity than Ni_{20}/Cu_{80}/CNTs at each temperature. That might be due to strong chemisorption of hydrogen on Ni particles to affect the catalytic activity of Ni/Cu/CNTs. When alloys of Ni and Cu were not formed, the strong adsorption of hydrogen on Ni reduced the contact of methanol with Ni; whereas, by the formation of Ni–Cu alloys, Cu atoms would interfere with the adsorption of hydrogen on Ni due to ensemble and ligand effects [25].

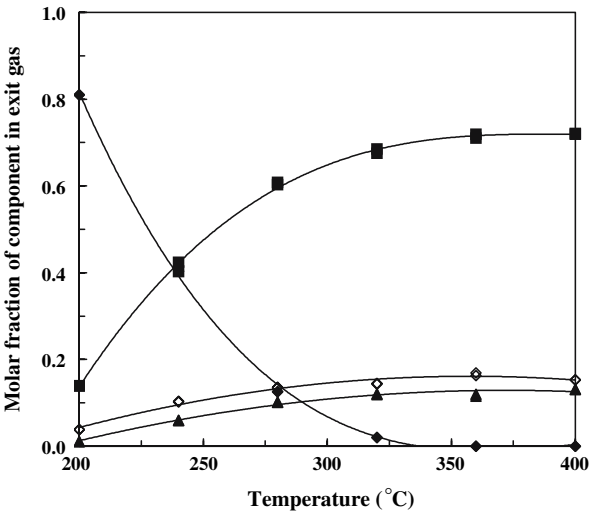

Fig. 7 Effect of reaction temperature on gas product distribution; 20 wt.% Cu_{20}–Ni_{80}/CNTs catalyst, 30.5 h of WHSV, 7 cm^3/h of Q, 1.5 of M, temperature at 200–400 °C, 80 cm^3/min of volumetric rate of nitrogen; (*filled diamond*) methanol, (*filled square*) hydrogen, (*filled triangle*) carbon monoxide, (*open diamond*) carbon dioxide

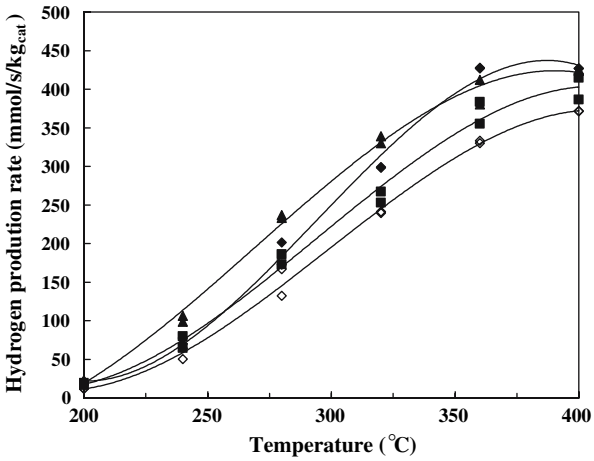

Fig. 8 Comparison of Ni_{20}–Cu_{80}/CNTs and Ni_{20}/Cu_{80}/CNTs on hydrogen production rate; 30.5 h of WHSV, 7 cm^3/h of Q, 1.5 of M, temperature at 200–400 °C, 80 cm^3/min of volumetric rate of nitrogen; (*filled diamond*) 28 wt.% Ni_{20}–Cu_{80}/CNTs, (*filled square*) 28 wt.% Ni_{20}/Cu_{80}/CNTs, (*filled triangle*) 20 wt.% Ni_{20}–Cu_{80}/CNTs, (*open diamond*) 20 wt.% Ni_{20}/Cu_{80}/CNTs

The comparison of a relative loading of Ni in 20 wt.% Ni_n–$Cu_{(100-n)}$/CNTs at 360 °C is shown in Table 5. The catalyst Ni_{20}–Cu_{80}/CNTs showed the highest activity with the highest yield and production rate of hydrogen. Obviously, a proper ratio of Ni to Cu in alloys was essential for steam reforming of methanol due to Ni and Cu catalyzing the reactions by different routes. The order for hydrogen production rate is Ni_{20}–Cu_{80}/CNTs > Ni/CNTs > Ni_{40}–Cu_{60}/CNTs ≈ Ni_{60}–Cu_{40}/CNTs > Ni_{80}–Cu_{20}/CNTs. The selectivity of CO_2 decreased with an increase of Ni percentage in Ni–Cu alloys, because a larger content of Ni can catalyze MD reaction more effectively to produce CO. Nevertheless, when the metal catalyst is Ni purely, the

Table 5 Effect of Ni content in 20 wt.% Ni_n–$Cu_{(100-n)}$/CNTs on steam reforming of methanol[a]

N	H_2 yield at 360 °C (%)	Maximum H_2 production rate (mmol H_2 s^{-1} kg_{cat}^{-1})	Selectivity of CO_2 (min/max, %)
100	83.6	415.6	56.8/63.9
80	74.9	359.4	48.1/69.1
60	83.7	387.4	50.2/61.7
40	79.4	385.2	51.9/76.2
20	98.6	425.2	53.8/77.7

[a] Reaction conditions: 0.2 g of catalyst, 30.5 h of WHSV, 7 cm^3/h of Q, 1.5 of M, temperature at 200–400 °C, 80 cm^3/min of volumetric rate of nitrogen

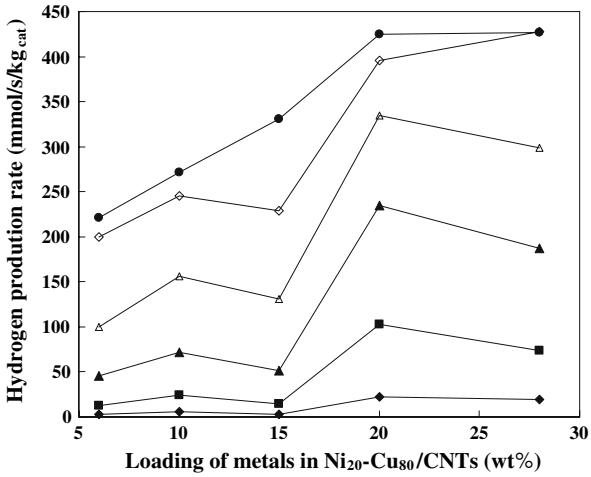

Fig. 9 Effect of total loading of alloys in Ni_{20}–Cu_{80}/CNTs on hydrogen production; 30.5 h of WHSV, 7 cm^3/h of Q, 1.5 of M, temperature at 200–400 °C, 80 cm^3/min of volumetric rate of nitrogen; temperature (°C): (*filled diamond*) 200, (*filled square*) 240, (*filled triangle*) 280, (*open triangle*) 320, (*open diamond*) 360, (*filled circle*) 400

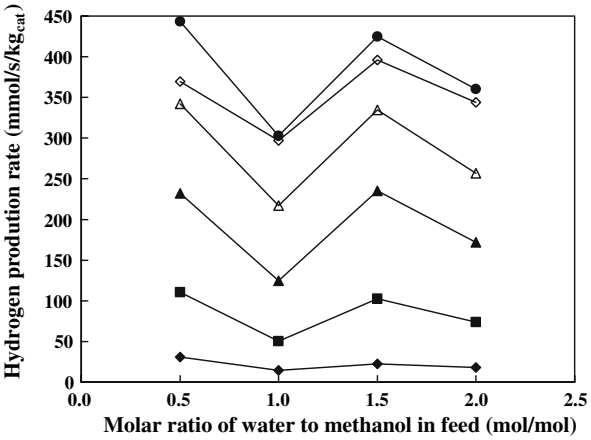

Fig. 10 Effect of molar ratio of water to methanol in feed on hydrogen production rate; 20 wt.% Ni_{20}–Cu_{80}/CNTs, 30.5 h of WHSV, 7 cm^3/h of Q, 1.5 of M, temperature at 200–400 °C, 80 cm^3/min of volumetric rate of nitrogen; temperature (°C): (*filled diamond*) 200, (*filled square*) 240, (*filled triangle*) 280, (*open triangle*) 320, (*open diamond*) 360, (*filled circle*) 400

WGS reaction of CO can progress more easily at a higher temperature to increase the selectivity of CO_2.

Figure 9 shows the effect of total loading of metals in Ni_{20}–Cu_{80}/CNT on hydrogen production. The results indicate that an optimal loading of alloys existed. A metal content between 20 and 28 wt.% for Ni_{20}–Cu_{80} alloy exhibited similar activity, and the hydrogen production increased with increasing the total loading of metals up to 20 wt.% at 400 °C; at a temperature lower than 360 °C, similar activities were observed for the loading between 6 and 15 wt.%. The larger content of alloys would supply more active sites, but a too large content might destroy the structures of CNTs, or induce serious aggregation of alloys [22]. At 360 °C, the hydrogen yield near 100% was achieved with a metal content >20 wt.% for Ni_{20}–Cu_{80}/CNT, as shown in Table 6. The maximum production rate of H_2 reached 425 mmol H_2 s/kg_{cat} with 77.7% of selectivity of CO_2 for 20 wt.% Ni_{20}-Cu_{80}/CNTs; while the selectivity of CO_2 varied not much for different loadings of alloys in Ni_{20}–Cu_{80}/CNTs.

The effect of *M*-value on hydrogen production at different temperatures over 20 wt.% Ni_{20}-Cu_{80}/CNTs is shown in Fig. 10. A similar tendency for hydrogen production was observed, and a minimum value located at *M* equal to 1. When *M*-value was <1, the MD reaction would be more significant because of a larger amount of methanol existing in the system; whereas, too large amount of water ($M = 2$) made a reduced rate of MD reaction. When *M*-value was >1, both the MD and WGS reactions were equally important.

Table 6 Effect of total loading of alloys in Ni_{20}–Cu_{80}/CNTs on steam reforming of methanol[a]

Loading of Ni_{20}–Cu_{80} (wt.%)	H_2 yield at 360 °C (%)	Maximum H_2 production rate (mmol H_2 s^{-1} kg_{cat}^{-1})	Selectivity of CO_2 (max/min, %)
28	96.8	427.0	68.4/60.1
20	98.7	425.3	77.7/53.8
15	53.0	338.9	78.0/60.4
10	53.7	280.0	80.0/61.2
6	45.9	228.3	76.7/57.1

[a] Reaction conditions: 0.2 g of catalyst, 30.5 h of WHSV, 7 cm^3/h of Q, 1.5 of M, temperature at 200–400 °C, 80 cm^3/min of volumetric rate of nitrogen

4 Conclusion

In this study, the novel catalyst Ni–Cu/CNTs was prepared and employed in steam reforming of methanol effectively. With the acid-treated CNTs, we successfully anchor the Ni–Cu alloys on CNTs by a simple reduction with formaldehyde. TMAOH plays an important role in dispersing the metal particles during the reduction under ultrasound shaking. The Ni–Cu alloys with an average size of 10–20 nm were obtained. The hydrogen yield near 100% was achieved at 360 °C with a metal loading between 20 and 28 wt.% of Ni_{20}–Cu_{80} alloy supported on CNTs. The catalyst 20 wt.% Ni_{20}–Cu_{80}/CNTs shows the highest activity than catalysts with 20 wt.% of metals in other Ni to Cu ratios. In comparison, the catalyst Ni–Cu alloys supported on activated carbon was also prepared by the similar procedures. It shows that the performance of Ni_{20}–Cu_{80}/CNTs on steam reforming of methanol is better than that of

Ni_{20}–Cu_{80}/C. Both the catalysts Ni/Cu/CNTs and Ni–Cu/CNTs showed good activities in steam reforming of methanol at 200–400 °C, but Ni–Cu alloys had a higher activity.

Acknowledgments The authors acknowledge the financial support of the National Science Council, Taiwan, Republic of China (Grant No. NSC 94-2214-E-005-011). This work is also supported in part by the Ministry of Education, Taiwan, Republic of China, under the ATU plan.

References

1. Lee JK, Ko JB, Kim DH (2004) Appl Catal A Gen 278:25
2. Karim A, Conant T, Datye A (2006) J Catal 243:420
3. Alejo L, Lago R, Pena MA, Fierro JLG (1997) Appl Catal A Gen 162:281
4. Matter PH, Ozkan US (2005) J Catal 234:463
5. Takezawa N, Iwasa N (1997) Catal Today 36:45
6. Wang Z, Xi J, Wang W, Lu G (2003) J Mol Catal A Chem 191:123
7. Suetsuna T, Suenaga S, Fukasawa T (2004) Appl Catal A Gen 276:275
8. Fukuhara C, Ohkura H, Kamata Y, Murakami Y, Igarashi A (2004) Appl Catal A Gen 273:125
9. Agrell J, Birgersson H, Boutonnet M, Melián-Cabrera I, Navarro RM, Fierro JLG (2003) J Catal 219:389
10. Ito S, Suwa Y, Konodo S, Kameoka S, Tomishige K, Kunimori K (2003) Catal Commun 4:499
11. Barthos R, Solymosi F (2007) J Catal 249:289
12. Wu GT, Wang CS, Zhang XB, Yang HS, Qi ZF, Li WZ (1998) J Power Sources 75:175
13. Serp P, Corrias M, Kalck P (2003) Appl Catal A Gen 253:337
14. Guczi L, Stefler G, Geszti O, Koppány Z, Kónya Z, Molnár É, Urbán M, Kiricsi I (2006) J Catal 244:24
15. Xu QC, Lin JD, Li J, Fu XZ, Yang ZW, Guo WM, Liao DW (2006) J Mol Catal A Chem 259:218
16. van der Lee MK, van Dillen AJ, Bitter JH, de Jong KP (2005) J Am Chem Soc 127:13573
17. Ma X, Li X, Lun N, Wen S (2006) Mater Chem Phys 97:351
18. Wang M, Woo KD, Kim DK (2006) Energy Conv Manag 470:3235
19. Liu H, Cheng G, Zheng R, Zhao Y, Liang C (2005) J Mol Catal A Chem 230:17
20. Ang LM, Hor TSA, Xu GQ, Tung CH, Zhao SP, Wang JLS (2000) Carbon 38:363
21. Yang HM, Liao PH (2007) Appl Catal A Gen 317:226
22. Feng J, Zhang CP (2006) J Colloid Interface Sci 293:414
23. Lindstrom B, Pettersson J, Menon PG (2002) Appl Catal A Gen 234:111
24. Agrell J, Birgersson H, Boutoneet M (2002) J Power Sources 106:249
25. Satterfield CN (1980) Heterogeneous catalysis in practice. McGraw-Hill, New York, p 132